

Undertow Velocity Induced by Irregular Waves

Winyu Rattanapitikon

Department of Civil Engineering, Sirindhorn International Institute of Technology, Thammasat University,
Klong Luang, Phatum Thani 12121, Thailand

Abstract

A simple model is developed for computing the undertow velocity induced by irregular waves. The present model is developed by applying the undertow model for regular waves. The main formula is derived from the eddy viscosity approach. The present model is calibrated by using published experimental data from 5 sources covering small-scale, large-scale and field experiments. All coefficients in the model are kept to be constant for all cases of computation. The model appears to give reasonable predictions of undertow velocity for wide range of experimental conditions.

1. Introduction

Cross-shore time-averaged velocity below wave trough, or undertow, is important in the computation of suspended sediment transport rate and consequently, beach deformation.

Cox and Kobayashi (1997) developed a model for computing the profile (vertical distribution) of undertow induced by regular waves. The model combines a logarithmic profile in the bottom boundary layer with a parabolic profile in the middle layer. Their model was applied by Kennedy et al. (1998) to predict the profile of undertow induced by irregular waves. Their model is simple and easy to use but the empirical coefficients in the model are not really constant. The coefficients have to be adjusted at each measured profile. This may be difficult to use in the practical work.

Recently, Rattanapitikon and Shibayama (2000) developed an undertow model for regular waves. The model is examined using published laboratory data from 6 sources covering small-scale and large-scale experiments. Unlike the model of Cox and Kobayashi (1997), all coefficients in the model are kept to be constant for all cases of computation. The model was found to give accurate predictions of the undertow velocity.

This paper extends Rattanapitikon and Shibayama (2000)'s work by applying the model to predict undertow velocity induced by irregular waves. Published experimental data of undertow profiles from 5 sources, including 675 undertow profiles, have been collected for calibration of the present model. These include small-scale, large-scale, and field experimental data obtained from a variety of wave and bottom conditions. A summary of the collected experimental data is given in Table 1.

This paper is organized as follows; the undertow model for regular waves of Rattanapitikon and Shibayama (2000) is briefly reviewed in the next section and the development of undertow model for irregular waves is described in section 3.

2. Undertow Model for Regular Waves

The undertow model for regular waves of Rattanapitikon and Shibayama (2000) is summarized herein to facilitate the comprehension of the subsequent comparisons. For more detail please see their paper.

2.1. Profile of undertow velocity induced by regular waves

The undertow profile is calculated from the eddy viscosity model:

$$\tau = \rho \nu_t \frac{\partial U}{\partial z} \quad (1)$$

where τ is the time-averaged shear stress, ρ is fluid density, ν_t is the time-averaged eddy viscosity coefficient, U is the time-averaged velocity or undertow, and z is the upward vertical coordinate from the bed.

Based on the experiment of Okayasu et al. (1988), the formula of τ / ν_t can be expressed as

$$\frac{\tau}{\nu_t} = \rho^{2/3} D_B^{1/3} \left[\frac{k_1}{d_t} + \frac{k_2}{z} \right] \quad (2)$$

where D_B is the energy dissipation rate of a broken wave, d_t is the water depth at wave trough, and k_1 and k_2 are the coefficients.

Substituting Eq. (2) into Eq. (1) then taking integration and using mean undertow velocity

$U_m = \frac{1}{d_i} \int_0^{d_i} U dz$ as the boundary condition, yields the result

$$U = \left(\frac{D_B}{\rho} \right)^{1/3} \left[k_1 \left(\frac{z}{d_i} - \frac{1}{2} \right) + k_2 \left(\ln \frac{z}{d_i} + 1 \right) \right] + U_m \quad (3)$$

According to the difference of observed breaking wave shape, Svendsen et al. (1978) suggested to divide the surf zone into transition zone and inner surf zone. The experimental results of Okayasu (1989) show that the turbulence, induced by breaking waves, in the transition zone is different from the inner surf zone. Since the mechanisms of turbulence induced by breaking wave (or surface roller) in these two zones are different, the different treatment is necessary. To incorporate the influence of the transition zone, for the sake of simplicity, Eq. (3) is written as

$$U = k_3 \left(\frac{D_B}{\rho} \right)^{1/3} \left[k_1 \left(\frac{z}{d_i} - \frac{1}{2} \right) + k_2 \left(\ln \frac{z}{d_i} + 1 \right) \right] + U_m \quad (4)$$

where k_3 is the coefficient introduced herein to account for the influence of transition zone.

From the bore model (Thornton and Guza, 1983), D_B can be expressed as

$$D_B = \frac{\rho g H^3}{4 T h} \quad (5)$$

where g is the acceleration of the gravity, H is the wave height, T is the wave period, and h is the mean water depth.

2.2. Mean undertow velocity induced by regular waves

The mean undertow velocity (U_m) is assumed to consist of two components, one is due to the wave motion and the other one due to the surface roller. The derivation of mean undertow velocity (U_m) is based on the re-analysis of existing formulas. The result is

$$U_m = -k_4 \frac{B_o g H^2}{c h} - k_5 \frac{B_o c H}{h} \quad (6)$$

where k_4 and k_5 are the coefficients, c is the phase velocity, $B_o = \frac{1}{T} \int_0^T \left(\frac{\eta}{H} \right)^2 dt$ is the wave shape

parameter which is equal to 1/8 for sinusoidal waves, η is the water surface elevation measured from mean water level, and t is time.

3. Undertow Model for Irregular Waves

Irregular wave is more complex than regular wave. In contrast to regular waves there is no well-defined breaking point for irregular waves. The highest wave tends to break at greatest distance from

the shore. Thus the turbulence, induced by irregular breaking waves, occurs over a considerably greater area than that of regular waves. Since the width of surf zone and the transition zone varies with each individual wave, the influence of the transition zone is not significantly observed in the irregular wave surf zone (Nairn et al., 1990). To make the model simple, the influence of the transition zone for irregular wave is excluded in this study.

The undertow model for regular waves (Eqs. 4-6) is applied to compute the undertow induced by irregular waves. The height and period of the irregular waves are represented by the root mean square wave height (H_{rms}) and peak spectral wave period (T_p).

3.1. Profile of undertow velocity induced by irregular waves

Excluding the effect of transition zone, Eq. (4) is applied for computing the undertow profile of irregular waves as

$$U = D_B^{1/3} \left[k_6 \left(\frac{z}{d_i} - \frac{1}{2} \right) + k_7 \left(\ln \frac{z}{d_i} + 1 \right) \right] + U_m \quad (7)$$

where k_6 and k_7 are the coefficients.

Using the concept of Battjes and Janssen (1978), Eq. (5) is modified for computing the energy dissipation rate of the irregular breaking waves as

$$D_B = \frac{Q_b \rho g H_{rms}^3}{4 T_p h} \quad (8)$$

where Q_b is the fraction of breaking wave which can be computed from the derivation of Battjes and Janssen (1978) as

$$\frac{1 - Q_b}{- \ln Q_b} = \left(\frac{H_{rms}}{H_b} \right)^2 \quad (9)$$

where H_b is the breaking wave height that can be computed by using breaking criteria of Goda (1970):

$$H_b = 0.1 L_o \left\{ 1 - \exp \left[-1.5 \frac{\pi h}{L_o} \left(1 + 15 m^{4/3} \right) \right] \right\} \quad (10)$$

where L_o is the deep-water wavelength related to peak spectral wave period, and m is the bottom slope. The coefficient 0.1 is used according to Rattanapitikon and Shibayama (1998).

Substituting Eq. (8) into Eq. (7), the undertow profile can be expressed as

$$U = \left(\frac{Q_b \rho g H_{rms}^3}{4 T_p h} \right)^{1/3} \left[k_6 \left(\frac{z}{d_i} - \frac{1}{2} \right) + k_7 \left(\ln \frac{z}{d_i} + 1 \right) \right] + U_m \quad (11)$$

The coefficients k_6 and k_7 can be determined from the formula calibration. The measured undertow profile data from 5 sources (see Table 1) are used to calibrate the formula.

In order to evaluate the accuracy of the prediction, the verification results are presented in term of root mean square relative error (ER) as:

$$ER = 100 \sqrt{\frac{\sum_{i=1}^{tn} (U_{ci} - U_{oi})^2}{\sum_{i=1}^{tn} U_{oi}^2}} \quad (12)$$

where i is the velocity number, U_{ci} is the computed velocity of number i , U_{oi} is the measured velocity of number i , tn is the total number of measured velocity.

The undertow profile is computed from Eq. (11) by using measured U_m as the input data. Trial simulations indicated that $k_6 = 0.30$ and $k_7 = 0.12$ give good agreement between measured and computed undertows. Table 2 shows the rms relative error (ER) for each case. The rms relative error (ER) for all cases is 20.5%. Fig. 1 shows the verification results of all measuring points. Fig. 2 shows the examples of measured and computed undertow profiles. Figs. 1-2 and Table 2 show that the Eq. (11) is accurate enough to be used for computing the profile (or shape) of undertows induced by irregular waves.

3.2. Mean undertow velocity induced by irregular waves

The formula of mean undertow velocity for regular waves (Eq. 6) is applied to irregular waves by the equivalent regular waves based on the root mean square wave height (H_{rms}) and peak spectral wave period (T_p). Excluding the effect of transition zone, Eq. (6) is modified to compute U_m of irregular waves as

$$U_m = -k_8 \frac{gH_{rms}^2}{c_p h} - k_9 \frac{Q_b c_p H_{rms}}{h} \quad (13)$$

where c_p is the phase velocity related to peak spectral wave period, and k_8 and k_9 are the coefficients which can be determined by the formula calibration.

The measured undertow profile data, under irregular wave actions, from 5 sources (see Table 1) are used to calibrate the formula. Trial simulations indicated that $k_8 = 0.57$ and $k_9 = 0.50$ give good agreement between measured and computed undertows. Table 3 shows the rms relative error (ER) for each data source. The rms relative error (ER) for all collected data is 42.6%. Fig. 3 shows the comparison between measured and computed mean undertow velocity. Figs. 4 and 5 show the examples

of cross-shore variations of measured and computed the mean undertow velocities.

To confirm the ability of the present formula (Eq. 13), the following sub-section presents the comparison between the present formula and the existing formulas.

3.2.1. Comparison with other formulas

From the previous studies, the following explicit formulas have been suggested to compute the mean undertow velocity induced by irregular wave actions:

Rodriguez et al. (1994) modified the formula of De Vriend and Stive (1987) to predict the mean undertow velocity induced by irregular wave actions:

$$U_m = -k_{R1} \frac{gH_{rms}^2}{8c_p d_t} - k_{R2} Q_b \frac{h}{L_p} \frac{gH_{rms}^2}{8c_p d_t} \quad (14)$$

where L_p is the wavelength related to peak spectral wave period, k_{R1} and k_{R2} are the coefficients. The published value of k_{R1} is 1.0, and k_{R2} is 7.0.

Grasmeijer and Van Rijn (1997) proposed:

$$U_m = -k_{G1} \sqrt{\frac{g}{h}} \frac{H_{rms}^2}{d_t} \quad (15)$$

where k_{G1} is the coefficient. The published value of k_{G1} is 0.125.

Kennedy et al. (1998) proposed:

$$U_m = -k_{K1} \frac{\sqrt{gh}}{8} \left(\frac{H_{rms}}{h} \right)^2 \quad (16)$$

where k_{K1} is the coefficient.

Using the collected experimental data from Table 1, the above 3 formulas (Eqs. 14-16) are re-calibrated to determine the best-fit coefficients in each formula. The verification results are presented in term of rms relative error (ER) and summarized in Table 4. It can be seen from Table 4 that the coefficients in the formulas of Rodriguez et al. (1994) and Grasmeijer and Van Rijn (1997) need to be slightly changed and the present formula (Eq. 13) shows the best prediction.

3.3. Recommended procedure for computing undertow velocity

The recommended procedure for computing undertow velocity, is summarized as follows:

- 1) Given z , d_t , h , H_{rms} , T_p , and m .
- 2) Compute c_p and L_p using linear wave theory.
- 3) Compute H_b , Q_b , and U_m from Eqs. (10), (9), and (13), respectively.
- 4) Compute U from Eq. (11).

4. Conclusions

The undertow model for regular waves was extended to predict the undertow velocity for irregular waves. The height and period of the irregular waves are represented by the root mean square wave height and peak spectral wave period. The description of undertow velocity is classified into two steps. The first step is to determine the undertow profile and the second step is to determine the mean undertow velocity. Published experimental data from 5 sources were used for calibrating the present model. The error (ER) of the formulas for computing undertow profile is 20.5% while the error of the formula computing mean undertow velocity is 42.6%. The previous formulas for computing mean undertow velocity were compared with the present formula. The comparison indicates that the present formulas give the best prediction.

Acknowledgment: This research is sponsored by the Thailand Research Fund.

References

[1] Battjes, J.A. and Janssen, J.P.E.M. (1978). Energy loss and set-up due to breaking of random waves, Proc. 16th Coastal Eng. Conf., pp. 569-587.

[2] Cox, D.T. and Kobayashi, N. (1997). Kinematic undertow model with logarithmic boundary layer, J. of Waterway, Port, Coastal, and Ocean Eng., Vol. 123, No. 6, pp. 354-360.

[3] De Vriend, H.J. and Stive, M.J.F. (1987). Quasi-3D modelling of nearshore currents. Coastal Eng., Vol. 11, pp. 565-601.

[4] Dette, H.H. and Uliczka, K. (1986). Velocity and sediment concentration fields across surf zones, Proc. 20th Coastal Eng. Conf., pp. 1062-1076.

[5] Grasmeijer, B.T. and Van Rijn L.C. (1997). Transport of fine sands by currents and waves. III: breaking waves over barred profile with ripples, J. of Waterway, Port, Coastal, and Ocean Eng., Vol. 125, No. 2, pp. 71-79.

[6] Goda, Y. (1970). A synthesis of breaking indices, Trans. JSCE., Vol. 2, Part 2, pp. 227-230.

[7] Kennedy, D.L., Cox, D.T. and Kobayashi, N. (1998). Application of an undertow model to irregular waves on barred beaches and reflective coastal structures, Proc. 26th Coastal Eng. Conf., pp. 311-324.

[8] Kraus, N.C. and Smith, J.M. (1994). SUPERTANK Laboratory Data Collection Project, Tech. Report CERC-94-3, U.S. Army Corps of Eng., WES, Vol. 1-2.

[9] Nairn R.B., Roelvink, J.A. and Southgate H.N. (1990). Transition zone width and implications for modelling surf zone hydrodynamics, Proc. 22nd Coastal Eng. Conf., pp. 68-81.

[10] Okayasu, A., Shibayama, T. and Horikawa, K. (1988). Vertical variation of undertow in the surf zone, Proc. 21st Coastal Eng. Conf., pp. 478-491.

[11] Okayasu, A. (1989). Characteristics of Turbulence Structure and Undertow in Surf Zone, D. Eng. Dissertation, U. of Tokyo, Japan.

[12] Okayasu, A. and Katayama, H. (1992). Distribution of undertow and long-wave component velocity due to random waves, Proc. 23rd Coastal Eng. Conf., pp. 883-893.

[13] Rattanapitikon, W. and Shibayama, T. (1998). Energy dissipation model for regular and irregular breaking waves, Coastal Eng. Journal (JSCE), Vol. 40, No. 4, pp. 327-346.

[14] Rattanapitikon, W. and Shibayama, T. (2000). Simple model for undertow profile, Coastal Eng. Journal (JSCE), Vol. 42, No. 1, pp. 1-30.

[15] Rodriguez, A., Arcilla, S.A., Collado, F.R., Gracia, V., Coussirat M.G. and Prieto, J. (1994). Wave and currents at the ebro delta surf zone: measurement and modelling, Proc. 24th Coastal Eng. Conf., pp. 2542-2556.

[16] Shimisu, T. and Ikeno, M. (1996). Experimental study on sediment transport in surf and swash zones using large wave flume, Proc. 25th Coastal Eng. Conf., pp. 3076-3089.

[17] Svendsen, I.A., Madsen, P.A. and Hansen, J.B. (1978). Wave characteristics in the surf zone, Proc. 16th Coastal Eng. Conf., pp. 520-539.

[18] Thornton, E.B. and Guza, R.T. (1983). Transformation of wave height distribution, J. Geophys. Res., Vol. 88, pp. 5925-5983.

Table 1: Summary of collected experimental data.

| No. | Sources | Total no. of cases | Total no. of profiles | Apparatus | Bed condition |
|-----|-----------------------------|--------------------|-----------------------|-------------|---------------|
| 1 | Dette and Uliczka (1986) | 1 | 4 | large-scale | sandy beach |
| 2 | Okayasu and Katayama (1992) | 1 | 6 | small-scale | plane beach |
| 3 | Kraus and Smith (1994) | 111 | 643 | large-scale | sandy beach |
| 4 | Shimisu and Ikeno (1996) | 4 | 14 | large-scale | sandy beach |
| 5 | Rodriguez et al. (1994) | 2 | 8 | field | sandy beach |
| | Total | 119 | 675 | | |

Table 2: Root mean square relative error (ER) of Eq. (11) comparing with the experiment performed under irregular wave actions.

| Sources | Test No. | Case No. | T (s) | H_i (cm) | h_i (cm) | Total No. of profiles | Total No. of points | ER (%) |
|-----------------------------|----------|--|---------|------------|------------|-----------------------|---------------------|----------|
| Dette and Uliczka (1986) | | dune without foreshore | 6.0 | 106.1 | 500 | 4 | 16 | 26.2 |
| Okayasu and Katayama (1992) | | 2 | 1.26 | 5.9 | 35 | 6 | 35 | 21.9 |
| Shimizu and Ikeno (1996) | | L2 | 5.0 | 76.4 | 205 | 3 | 15 | 19.6 |
| | | L3 | 5.0 | 83.4 | 205 | 3 | 15 | 31.0 |
| | | L5 | 3.0 | 73.5 | 200 | 4 | 14 | 23.1 |
| | | L6 | 3.0 | 77.1 | 200 | 4 | 14 | 20.6 |
| Rodriguez et al. (1994) | | C3 | 6.1 | 60 | 750 | 3 | 11 | 15.3 |
| | | C4 | 5.6 | 44.3 | 750 | 5 | 20 | 21.3 |
| Kraus and Smith (1994) | ST10 | a0509a, a0510a, a0512a, a0515a, a0517a, a0608a, a0609a, a0611a, a0615a | 3.0 | 56.6 | 305 | 53 | 118 | 23.9 |
| | | a0617a, a1618a | 3.0 | 56.6 | 290 | 12 | 29 | 31.5 |
| | | a0710a, a0711a, a0713a, a0715a, a0717a, a0808a, a0809a, a0812a, a0814a, a0815a | 4.5 | 56.6 | 305 | 60 | 139 | 25.6 |
| | | a0908a | 6.0 | 56.6 | 305 | 6 | 15 | 18.3 |
| | | a0910a | 5.0 | 35.4 | 305 | 6 | 18 | 20.5 |
| | | a0911a | 3.0 | 49.5 | 305 | 6 | 17 | 30.0 |
| | | a0912a | 3.0 | 63.6 | 305 | 6 | 15 | 31.3 |
| | | a0914a | 4.5 | 63.6 | 305 | 6 | 14 | 27.3 |
| | ST20 | a1212a | 8.0 | 28.3 | 305 | 6 | 13 | 11.0 |
| | | a1215a | 8.0 | 42.4 | 305 | 7 | 14 | 20.5 |
| | | a1217a | 8.0 | 56.6 | 305 | 6 | 10 | 23.3 |
| | | a1310a | 3.0 | 28.3 | 305 | 5 | 11 | 11.2 |
| | | a1313a | 3.0 | 42.4 | 305 | 7 | 13 | 27.7 |
| | | a1315a | 3.0 | 56.6 | 305 | 7 | 13 | 32.2 |
| | ST30 | a1408a, a1409a, a1410a, a1411a, a1413b | 8.0 | 28.3 | 305 | 31 | 58 | 8.9 |
| | | a1415a, a1416a, a1417a | 8.0 | 35.4 | 305 | 21 | 37 | 15.2 |
| | | a1507b, a1508a, a1510a, a1511a, a1513b | 9.0 | 28.3 | 305 | 32 | 50 | 10.0 |
| | | a1515a, a1516a | 9.0 | 35.4 | 290 | 14 | 18 | 20.4 |
| | | a1607b | 6.0 | 28.3 | 305 | 7 | 10 | 10.8 |
| | | a1608a | 7.0 | 35.4 | 305 | 7 | 10 | 12.2 |
| | | a1610a | 7.0 | 28.3 | 305 | 7 | 10 | 15.0 |
| | | a1611a | 10.0 | 28.3 | 305 | 7 | 10 | 13.5 |

Table 2 (cont.): Root mean square relative error (ER) of Eq. (11) comparing with the experiment performed under irregular wave actions.

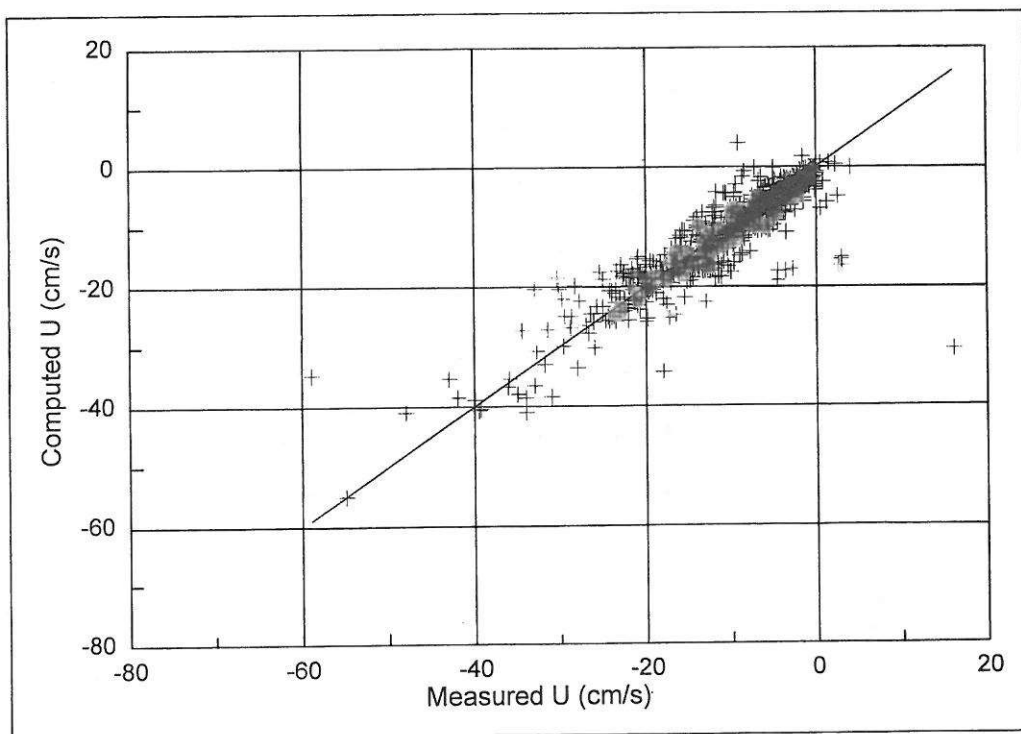
| Sources | Test No. | Case No. | T (s) | H_i (cm) | h_i (cm) | Total No. of profiles | Total No. of points | ER (%) | |
|------------------------|----------|--|---------|------------|------------|-----------------------|---------------------|--------|--|
| Kraus and Smith (1994) | ST40 | a1909b | 3.0 | 28.3 | 305 | 5 | 7 | 12.0 | |
| | | a2007b | 5.0 | 49.5 | 305 | 5 | 7 | 18.9 | |
| | | a2008a | 5.0 | 49.5 | 305 | 5 | 7 | 21.6 | |
| | | a2015a | 5/8 | 35.4 | 305 | 5 | 6 | 7.7 | |
| | | a2017a | 8.0 | 35.4 | 305 | 5 | 8 | 13.6 | |
| | | a2018a | 5.0 | 35.4 | 305 | 5 | 8 | 16.8 | |
| | | a2107b | 5/8 | 49.5 | 305 | 5 | 6 | 7.0 | |
| | | a2108a | 5/8 | 49.5 | 305 | 5 | 6 | 8.7 | |
| | | a2109a | 3/7 | 49.5 | 305 | 5 | 6 | 5.8 | |
| | | a2111a | 3/7 | 28.3 | 305 | 5 | 8 | 14.3 | |
| | | a2112a | 3/7 | 49.5 | 305 | 5 | 6 | 5.5 | |
| ST50 | ST50 | a2208a, a2209a | 3.0 | 56.6 | 290 | 10 | 12 | 5.8 | |
| | | a2209b | 4.5 | 56.6 | 290 | 5 | 7 | 7.9 | |
| | | a2210a | 6.0 | 56.6 | 290 | 6 | 8 | 3.3 | |
| | | a2213b | 3.0 | 56.6 | 320 | 7 | 14 | 19.8 | |
| | | a2214a | 4.5 | 49.5 | 320 | 7 | 14 | 18.0 | |
| | | a2215a | 6.0 | 49.5 | 320 | 6 | 13 | 15.6 | |
| | | a2216a | 3/7 | 35.4 | 320 | 7 | 14 | 21.7 | |
| | | a2308a, a2308b, a2309a | 3.0 | 49.5 | 320 | 18 | 39 | 16.5 | |
| | | | 4.5 | 49.5 | 320 | 18 | 39 | 15.3 | |
| | | | 6.0 | 35.4 | 335 | 15 | 41 | 21.6 | |
| ST70 | ST70 | a2609a, a2610a, a2610b | 4.5 | 49.5 | 290 | 12 | 18 | 5.8 | |
| | | a2613a | 4.5 | 49.5 | 305 | 4 | 6 | 9.4 | |
| | | a2614a, a2615a | 4.5 | 70.7 | 305 | 11 | 15 | 6.6 | |
| | | a2617b | 4.5 | 56.6 | 335 | 7 | 14 | 11.7 | |
| | | a2618a, a2618b | 4.5 | 49.5 | 335 | 14 | 28 | 11.7 | |
| | | a2708a, a2708b, a2709a | 4.5 | 49.5 | 335 | 20 | 31 | 31.8 | |
| ST90 | ST90 | | 3.0 | 49.5 | 335 | 20 | 38 | 22.3 | |
| | | | 3.0 | 49.5 | 335 | 7 | 14 | 17.8 | |
| STAO | STAO | a2816b | 3.0 | 49.5 | 335 | 12 | 22 | 9.6 | |
| | | s0209b, s0210a, s0211a | 3.0 | 56.6 | 274 | 15 | 25 | 10.7 | |
| | | | 3.0 | 49.5 | 305 | 18 | 41 | 20.6 | |
| STCO | STCO | s0913a, s0914a, s0915a, s0916a | 3.0 | 49.5 | 305 | 30 | 63 | 14.3 | |
| | | s0917a, s1008a, s1008b, s1009a, s1011a, s1013a | 8.0 | 35.4 | 305 | 675 | 1373 | 20.5 | |

Table 3: Summary of the *rms* relative error (*ER*) of the Eq. (13) for each data source.

| No. | Sources | Total no. of profiles | Apparatus | <i>ER</i> (%) |
|-----|-----------------------------|-----------------------|-------------|---------------|
| 1 | Dette and Uliczka (1986) | 4 | large-scale | 27.2 |
| 2 | Okayasu and Katayama (1992) | 6 | small-scale | 28.8 |
| 3 | Kraus and Smith (1994) | 643 | large-scale | 43.7 |
| 4 | Shimizu and Ikeno (1996) | 14 | large-scale | 30.3 |
| 5 | Rodriguez et al. (1994) | 8 | field | 48.9 |
| | Total | 675 | | 42.6 |

Table 4: Best-fit coefficients and verification results of the formulas of mean undertow velocity (measured data from Table 1).

| Formulas | Best-fit coefficients | | <i>ER</i> (%) |
|---|-----------------------|-----------------|---------------|
| | k_{m1} | k_{m2} | |
| Present Study (Eq. 13): | $k_g = 0.57$ | $k_0 = 0.50$ | 42.6 |
| Rodriguez et al., 1994 (Eq. 14): | $k_{R1} = 0.47$ | $k_{R2} = 4.92$ | 56.1 |
| Grasmeijer and Van Rijn, 1997 (Eq. 15): | $k_{G1} = 0.09$ | - | 58.0 |
| Kennedy et al., 1998 (Eq. 16): | $k_{K1} = 1.20$ | - | 47.0 |

Figure 1: Comparison between measured and computed the undertow velocity (*U*) in which the mean undertow velocity (U_m) is given data (measured data from Table 1).

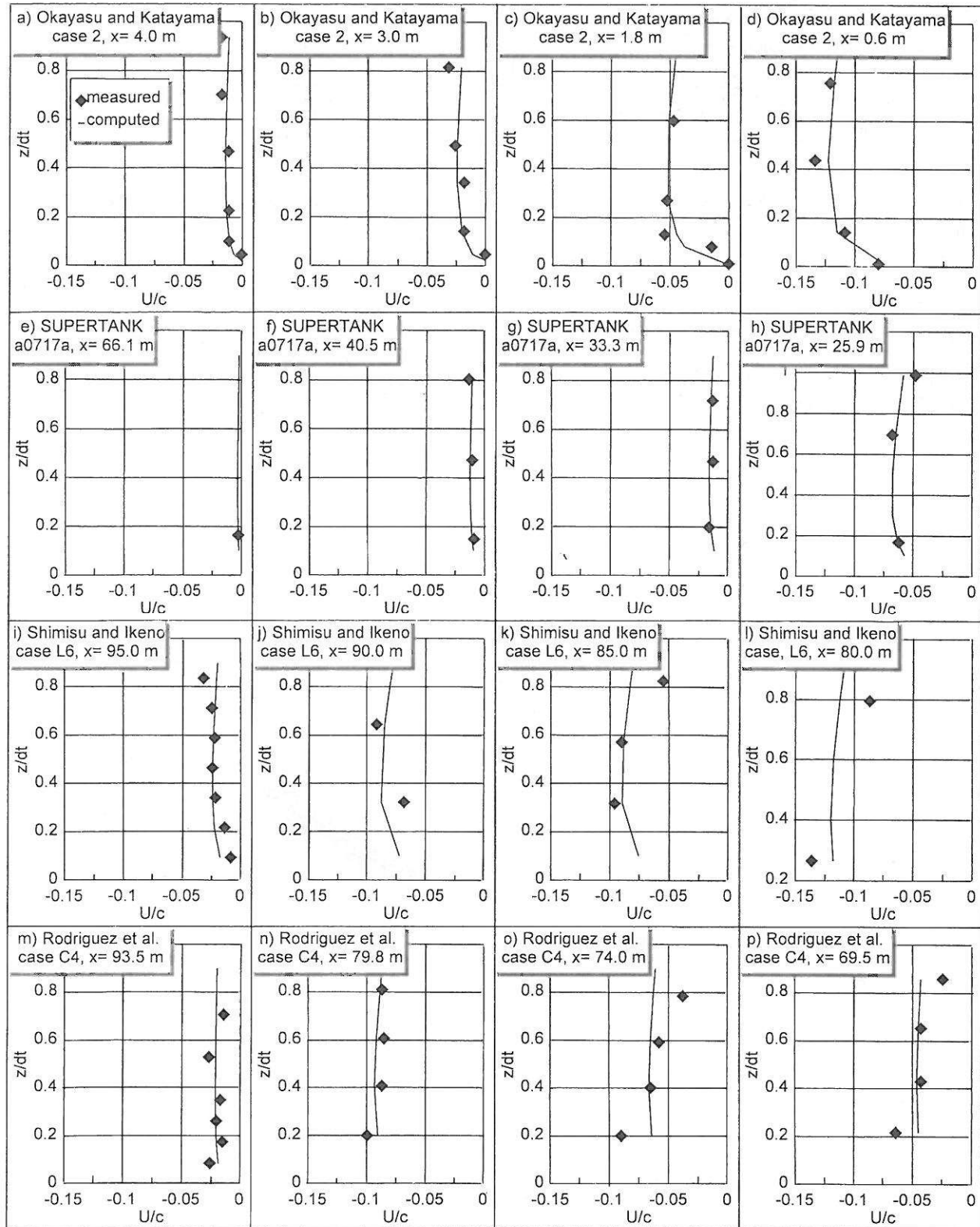


Figure 2: Examples of measured and computed undertow profiles in which the mean undertow velocity (U_m) is given data (measured data from Table 1).

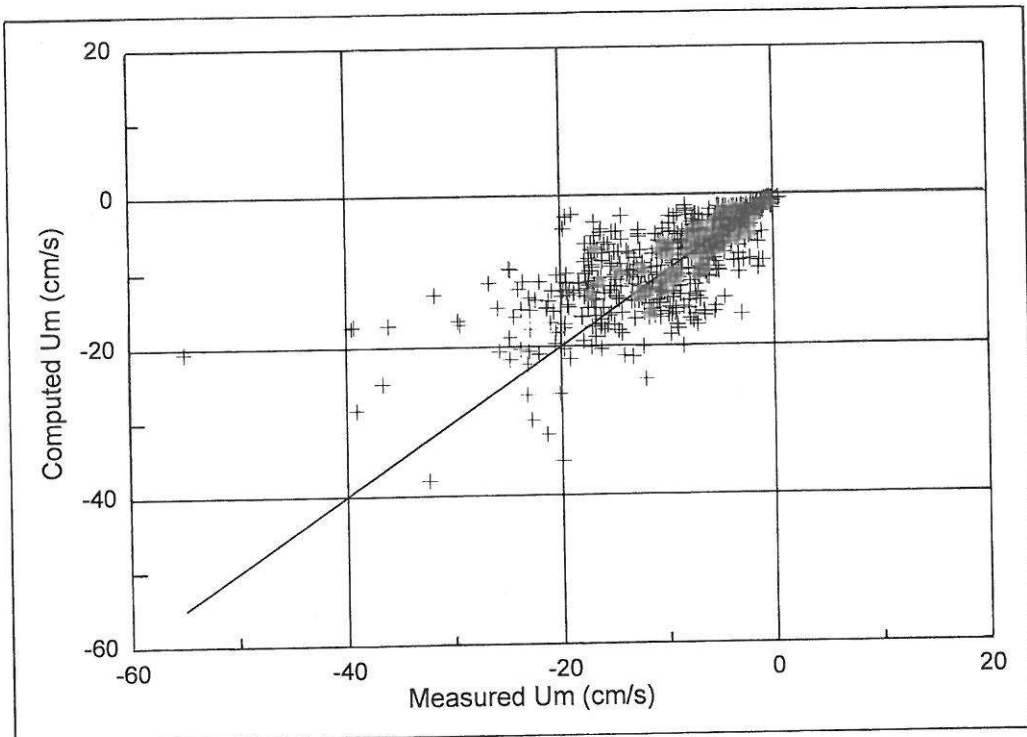


Figure 3: Comparison between measured and computed mean undertow velocity (U_m) induced by irregular wave actions (measured data from Table 1).

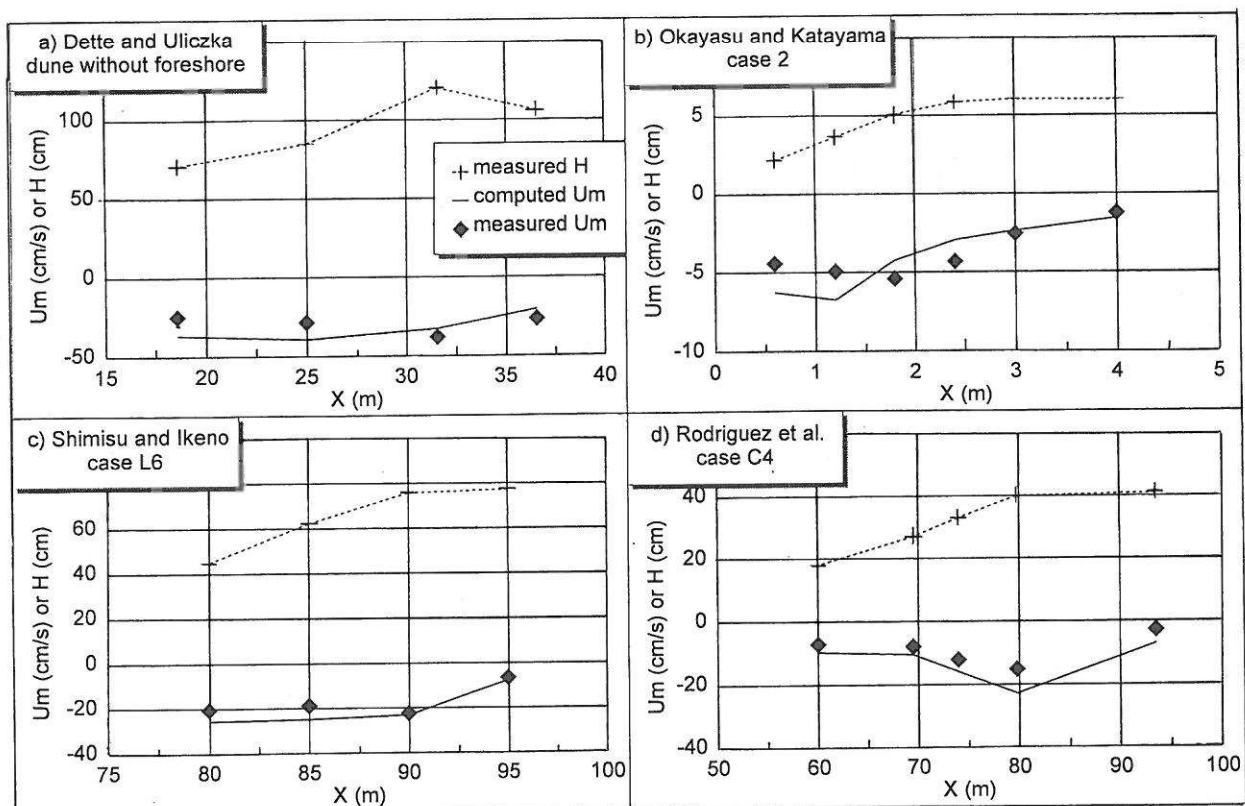


Figure 4: Examples of cross-shore variations of measured and computed mean undertow velocity (U_m) induced by irregular wave actions (measured data from Table 1, except the data of Kraus and Smith, 1994).

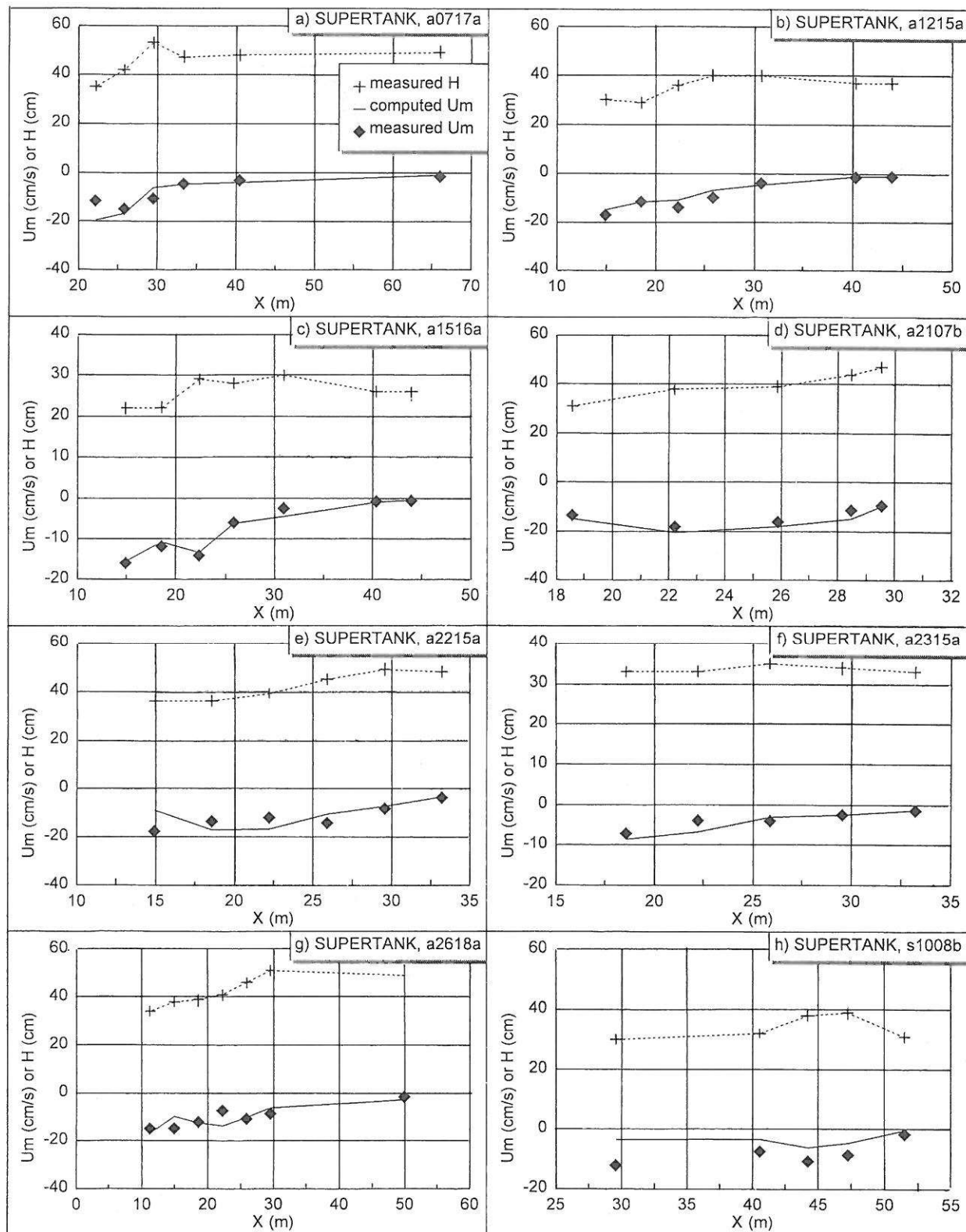


Figure 5: Examples of cross-shore variations of measured and computed mean undertow velocity (U_m) induced by irregular wave actions (measured data from Kraus and Smith, 1994).